Diagnosing the Airflow Mechanism of Blowhole Cave, Edwards County, Texas: A Quantitative Test of the Thermal-Chimney Model

Greg Passmore

Abstract

In late summer 1976, I recorded outside air temperature and signed entrance airflow at hourly intervals during five consecutive days at Blowhole Cave, Edwards County, Texas, with a return visit two weeks later that captured a continuous overnight cycle. The dataset comprises 96 hourly samples taken with a vane anemometer at a 0.139 m² (1.5 ft²) entrance restriction, with cave-air temperature independently measured at 22.2 °C (72 °F). I test the two dominant cave-ventilation hypotheses against these data. The buoyancy-driven thermal-chimney model fits the signed flow with a Pearson correlation of $r = +0.55$ against $\mathrm{sign}(\Delta T)\sqrt{|\Delta T|}$, with negligible correlation against dT/dt, and yields an effective chimney height $\Delta h \approx 49$ m (159 ft) from a single-parameter regression. The flow reverses sign precisely when outside temperature crosses cave temperature, a parameter-free prediction of the chimney model that no other mechanism reproduces. The 102 m (336 ft) of vertical relief surveyed inside the cave is more than sufficient to account for the observed flow. The barometric / large-volume hypothesis is rejected on six independent grounds, including a hidden-volume requirement of 1.6×10^7 m³, or roughly 1,100 times the surveyed cave volume. The result confirms the qualitative field interpretation recorded by the 1976 Project Deep survey team. The analysis extends the original treatment in Passmore (2023) with signed-flow analysis, USGS 3DEP topographic verification, and contextualization against the post-2020 cave-ventilation literature.

Introduction

Blowhole Cave lies on the Edwards Plateau of southwest Texas, on the Flat Rock 15-minute quadrangle in Edwards County. The entrance sits in a small draw at an elevation of 612 m (2,006 ft), in gently rolling limestone country mapped during the 1970s by the Project Deep survey team. The surveyed cave is 1,839 m (6,033 ft) long and 102.3 m (336 ft) deep (Pate and others, 1979), developed in Edwards Plateau limestones. The cave has considerable breakdown, making mapping (and exploring) complicated, and there are still unexplored areas.

The entrance is a hole approximately 0.46 m (1.5 ft) on each side at the bottom of the draw. Just inside, the passage widens and slopes downward at 12°. After 6 m (20 ft) of crawling, a steep drop leads into the first room, then a chimney climbs to a second room, then a series of pits leads down through breakdown to deeper rooms and finally to a 24 m (80 ft) pit. The cave's vertical extent is entirely below grade, organized as a stack of connected vertical airspaces threaded through the limestone. Internal rooms reach 30 by 24 m (100 by 80 ft) in plan with ceilings 18 to 21 m (60 to 70 ft) high. The 1976 survey team also recovered mammal bones from one of the deepest rooms, tentatively identified in the field as bear, which I note only as a historical observation; the airflow analysis does not depend on it.

When the survey team first measured the airflow, they wrote in their field notes that very strong currents flow from the cave during the afternoon and evening, while air enters the cave during the night and morning. They concluded, from the topographic setting and the diurnal sign reversal, that the present entrance is the lower opening of a two-entrance chimney system. They were right. The purpose of this paper is to show, quantitatively, how right.

A brief disambiguation is in order. The name Blowhole has been attached to at least two unrelated caves in the United States. The cave studied here is the Edwards County, Texas cave. A separate cave, Wupatki Blowhole No. 3e in Arizona, is a textbook example of single-entrance barometric ventilation, with an inferred volume of approximately

2×10^8 m³ (7 billion cubic feet) from breathing magnitude alone (Sartor and Lamar, 1962; Lewis, 1991). The two caves share a name and belong to opposite morphological classes.

This paper extends the original mathematical treatment of the 1976 dataset in Passmore (2023) with three additions: signed-flow analysis, in which outflow and inflow are treated with opposite sign rather than as magnitudes; USGS 3DEP elevation modeling of the cave footprint and surroundings; and contextualization against the cave-ventilation literature published since 2020. Methods cover the two competing physical mechanisms and the field data. Results give the diagnostic tests against the data, the topographic verification, and the rejection of the barometric alternative. Discussion treats the implications for the cave-ventilation literature and the limitations of the present analysis.

Methods

Candidate mechanisms

A cave breathes for one of a small number of physical reasons. For a karst cave in central Texas in summer, two candidates dominate the literature, and the cave's morphology decides which one prevails.

Thermal-chimney flow. Consider two openings at different elevations, separated vertically by Δh, connecting a cave interior at temperature T_c to an atmosphere at temperature T_o. Both columns of air feel the same surface pressure at their top. The cave interior, isothermal to first order, has air of one density; the matching column of outside air has air of another. Whichever column is denser sits with more weight on the lower opening, and the pressure difference at the lower opening drives flow until the two columns reach the same hydrostatic head. The driving pressure follows from the hydrostatic balance of two ideal-gas columns, and after the small $\Delta T / T$ simplification it reads

$$\Delta P_{\mathrm{buoy}} = \rho_o \, g \, \Delta h \, \frac{T_o - T_c}{T_o} = \rho_o \, g \, \Delta h \, \frac{\Delta T}{T_o}. \quad (1)$$

Equation (1) is exact only to leading order in $\Delta T / T$. At Blowhole, the ratio $|\Delta T| / T_o$ never exceeds 0.05, so the simplification carries a worst-case error of about 3 percent. Covington and others (2021), in their three-year record at Blowing Springs Cave in Arkansas, write the same expression with ρ_{in} in the prefactor and T_{ext} in the denominator. The two forms differ at second order and are interchangeable in practice.

The buoyancy head dissipates through every restriction inside the cave, but at Blowhole the entrance is the only severe restriction in series with much larger inner passages. Lumping every loss into a single discharge coefficient C_d, and equating ΔP_{buoy} to the dynamic-pressure loss $\tfrac{1}{2}\rho_o v^2 / C_d^2$ at the entrance, gives

$$v = C_d \sqrt{2 \, g \, \Delta h \, \frac{\Delta T}{T_o}}. \quad (2)$$

The factor of 2 inside the radical comes from inverting the half ρv^2 dynamic-pressure term. Massey (1989, *Mechanics of Fluids*) gives conventional values of C_d: approximately 0.61 for a sharp-edged orifice, 0.85 for a rounded short-tube opening into a larger volume, and 0.95 to 0.97 for a smooth nozzle. The Blowhole entrance is a small hole opening into rooms 10 to 100 times wider, geometry closer to a short converging nozzle than to a long pipe. I use $C_d = 0.65$ throughout, because that value is conservative for this geometry and biases the inferred Δh upward rather than downward. Covington and others (2021) and Gabrovšek and others (2021) instead split the loss term using Darcy-Weisbach, with friction factor f, passage length L, hydraulic diameter D_H, and minor-loss coefficients K_i. Their form is mathematically identical to Eq. (2) under the substitution $C_d^{-2} = (f L / D_H + \sum K_i)$. The distinction is bookkeeping.

The sign of v in Eq. (2) follows the sign of ΔT. When the outside is warmer than the cave, dense cave air spills out the lower entrance as outflow, taken as positive. When the outside is colder, the column reverses, and surface air falls into

the cave as inflow, taken as negative. Three testable predictions follow. First, signed flow tracks $\mathrm{sign}(\Delta T)\sqrt{|\Delta T|}$ and reverses precisely when outside temperature crosses cave temperature. Second, flow correlates with absolute temperature, not with its time derivative. Third, the magnitude-to-ΔT scaling is fixed by Δh, which is recoverable from a single regression.

Barometric flow. A different cave morphology produces a different mechanism. Take a cave with a single opening, or several openings at the same elevation, and a very large internal volume V. Outside pressure changes force air in and out of the cavity to maintain mass balance. Conservation of mass with adiabatic compression gives, to first order,

$$v = -\frac{V}{A\,P}\,\frac{dP}{dt}, \quad (3)$$

where A is the entrance area and P is the absolute atmospheric pressure. Equation (3) treats the cave as an incompressible reservoir. A more careful treatment retains compressibility and gives a Helmholtz oscillator with a natural frequency, but the synoptic forcing of interest here is slow enough that the quasi-static form suffices. Gomell and Pflitsch (2022), working at Wind Cave and Jewel Cave in South Dakota, refined the barometric picture by showing that the relevant predictor for airflow is the pressure gradient between cave interior and surface, not the surface-pressure rate of change in isolation. Three predictions follow from the barometric model. First, flow correlates with the pressure derivative, not with absolute outside temperature. Second, sign reversals lock to the pressure-forcing timescale, which for synoptic systems is 12 to 36 hours and is unrelated to time of day. Third, any temperature correlation arises only indirectly, through the weak coupling between P and T that passing fronts produce.

Simultaneous pressure data were not collected at Blowhole during the 1976 measurements. The barometric hypothesis therefore cannot be tested directly. It does, however, make several predictions about the temperature relationship that are falsifiable with the data on hand, and that is the line of attack used here.

Context from the literature

The framework above is consistent with four decades of cave-ventilation work. de Freitas and others (1982), using sulfur hexafluoride and CCl_2F_2 tracer gas at Glowworm Cave in New Zealand, established the modern reading that cave ventilation is driven by thermally induced air-density disequilibrium. Christoforou and others (1996) developed a quantitative natural-convection model for the multi-opening Buddhist cave temples at Yungang in China, demonstrating that outdoor-to-interior temperature differences alone suffice to predict ventilation rates in two-entrance temperature-driven geometries. The Yungang grottoes are shallow excavations with multiple large openings rather than vertically stacked karst caves, but the mathematical framework is identical to Eq. (2).

Faimon and Lang (2013), working at the U-shaped Císařská Cave in the Moravian Karst, reported a refinement that matters directly for the Blowhole analysis. The chimney airflow magnitude is linear in air-density difference but nonlinear in temperature difference, because air density is itself nonlinear in temperature. They also observed that upward airflows are systematically faster than downward airflows under comparable driving forces, through a positive feedback between external temperature and the rising buoyancy column, with a corresponding negative feedback on the descending side. I return to this asymmetry below, where it explains a substantial fraction of the unmodeled variance in the Blowhole regression.

More recent work extends the picture in two further directions. Gabrovšek (2023) presented a numerical model of a passage thermally coupled to the surrounding rock mass and showed that the effective T_c varies along a thermal-relaxation length over which entering air equilibrates with the rock. Sedaghatkish and others (2024) extended this with a parametric study and reported that the convective length scales approximately as airflow amplitude divided by the square root of cave radius. For Blowhole's dimensions and observed flow rates, this length is on the order of 100 m, which is comparable to the cave's surveyed horizontal extent. The deep cave is therefore approximately isothermal at a value close to the local mean annual surface temperature, a result that traces back to Wigley and Brown (1976) for the

general karst case. The measured 22.2 °C (72 °F) at Blowhole is consistent with this picture. The long-term mean annual temperature for Edwards County is approximately 18 °C (65 °F) (NOAA NCEI, 2024; Texas State Historical Association, 2024), and the excess of about 4 °C over the regional mean is the typical signature of a cave whose entry zone has been warmed by through-ventilation during the hot months.

Finally, Gabrovšek and others (2021) showed at Postojna Cave in Slovenia that wind flow over irregular surface topography can create pressure differences between cave entrances that augment, reduce, or even reverse the density-driven flow. For Blowhole's small entrance tucked at the bottom of a draw, surface-wind effects are likely modest. They are, however, a real source of unmodeled variance.

Data acquisition

James Thomas, Tom Mills and I made the measurements over six dates in the late summer of 1976. The first block covers five consecutive days, the 27th through the 31st of one month. The second block is a return visit on the 9th and 10th of the following month and captures a continuous overnight cycle. Each hourly observation records the hour of day in local time, the outside air temperature at the entrance in degrees Fahrenheit (converted to degrees Celsius for the analysis), and the entrance wind speed in feet per minute (converted to meters per second). Wind direction is signed, with positive values for outflow leaving the cave and negative for inflow entering it.

Cave-air temperature was measured independently at 22.2 °C (72 °F), taken with a glass thermometer in the deep rooms after sufficient dwell time for the instrument to equilibrate. The entrance restriction is a rectangular opening 0.30 m tall by 0.46 m wide (12 in by 18 in), area 0.139 m² (1.5 ft²). The anemometer was a vane-type handheld instrument with approximately ±0.25 m/s (±50 ft/min) resolution at the low end of its scale and roughly 10 percent accuracy at typical readings. The absolute calibration cannot be retrieved at this remove.

The full dataset contains 96 hourly samples. Outside temperatures range from 20.0 to 36.7 °C (68 to 98 °F). Signed wind ranges from -2.08 to $+8.00$ m/s (-410 to $+1575$ ft/min). Of the 96 samples, 67 show outflow above 0.25 m/s (50 ft/min), 20 show inflow below -0.25 m/s, and 9 are near zero.

Topographic analysis

Surface topography around the cave was characterized using the USGS 3D Elevation Program (3DEP) National Elevation Dataset, accessed in 2026. A 31-by-31 grid of elevation samples at 200 m spacing was extracted centered on the cave entrance, giving 961 samples covering a 6 km box. Maximum surface elevation within concentric radii from the entrance was tabulated to characterize the available relief that could support a second exchange opening above the present entrance.

Results

Sign and phase of reversals

The pattern of airflow is visible by inspection (Fig. 1). Outflow ramps up through late morning, peaks in the late afternoon between 16:00 and 19:00, and decays through evening. Inflow takes over overnight, peaks in the small hours of the morning, and ends near sunrise. The continuous overnight block on the 9th and 10th captures the reversal explicitly: from $+5.6$ m/s ($+1100$ ft/min) at 19:00 through zero near 21:00 to a sustained -1.0 to -2.0 m/s through the night, returning to outflow only after 09:00 the next morning. Covington and others (2021) document the same daily downdraft and nightly updraft pattern at Blowing Springs Cave in summer.

Aggregating the signed wind by hour of day across all observation days yields the diurnal composite (Fig. 2). The mean outside temperature crosses the cave temperature of 22.2 °C at approximately 08:00 in the morning and again near 21:30 in the evening. The mean signed wind shows a robust evening reversal at 21:37 local time, where multiple samples on multiple days transition from outflow to inflow. The corresponding morning reversal is not robustly sampled in the composite because most measurement days began at or after 08:00, when the cave was already in the outflow regime. The single continuous overnight block on the 9th and 10th, which is the only record that captured an

unbroken transition through both reversals, shows the evening reversal between 20:00 and 21:00 and the morning reversal between 08:00 and 09:00. Both crossings happen where the chimney model predicts they should, with no fitted parameter.

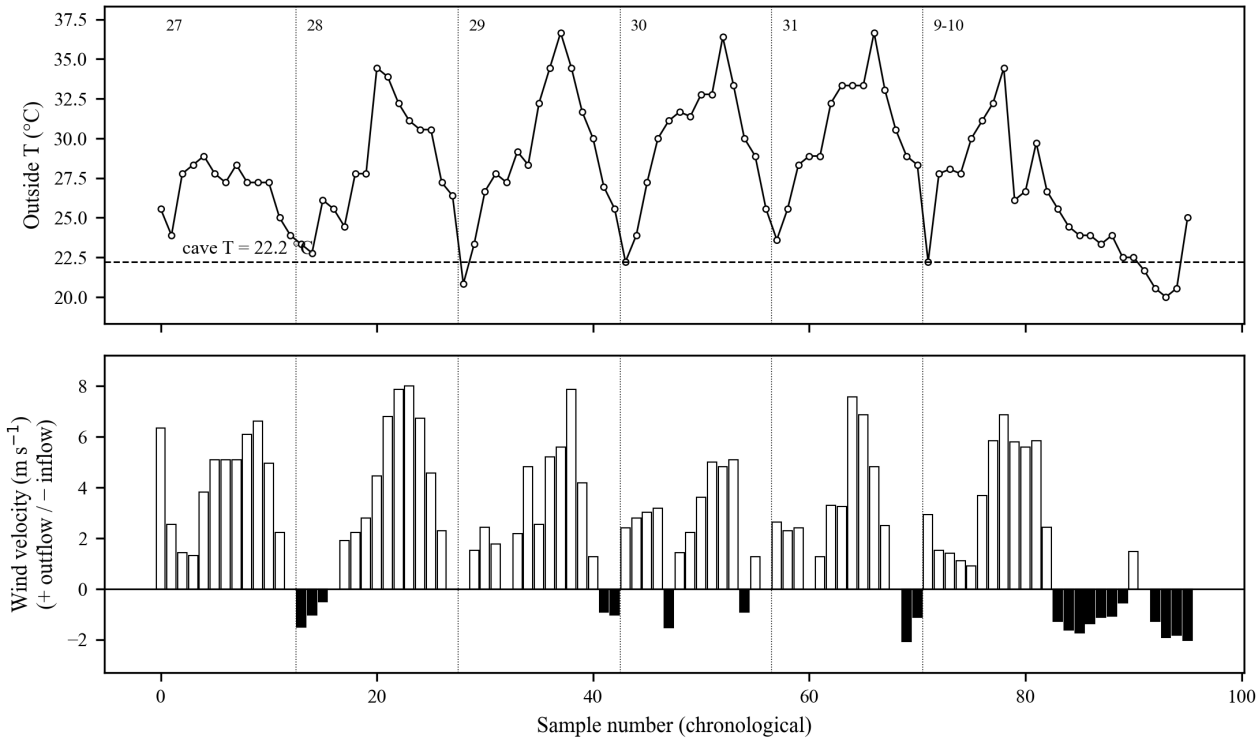

Figure 1. Time series of outside air temperature (upper panel) and signed entrance airflow (lower panel) across the six observation dates in late summer 1976. Positive flow indicates outflow from the cave; negative flow indicates inflow. Cave-air temperature of 22.2 °C is marked as a dashed horizontal line in the upper panel. Vertical separators indicate day boundaries.

The hourly histograms of flow direction are equally clean. Outflow events concentrate in 09:00 through 20:00, with four to six samples in every daytime hour and zero in any night hour. Inflow events concentrate in 21:00 through 10:00, with peak occurrence in 22:00 through 24:00, the coolest hours of the night. The barometric mechanism predicts no such time-of-day lock. Pflitsch and others (2010) document for Wind and Jewel Caves that barometric airflow direction follows synoptic pressure systems on multi-day timescales with no diurnal phase relationship.

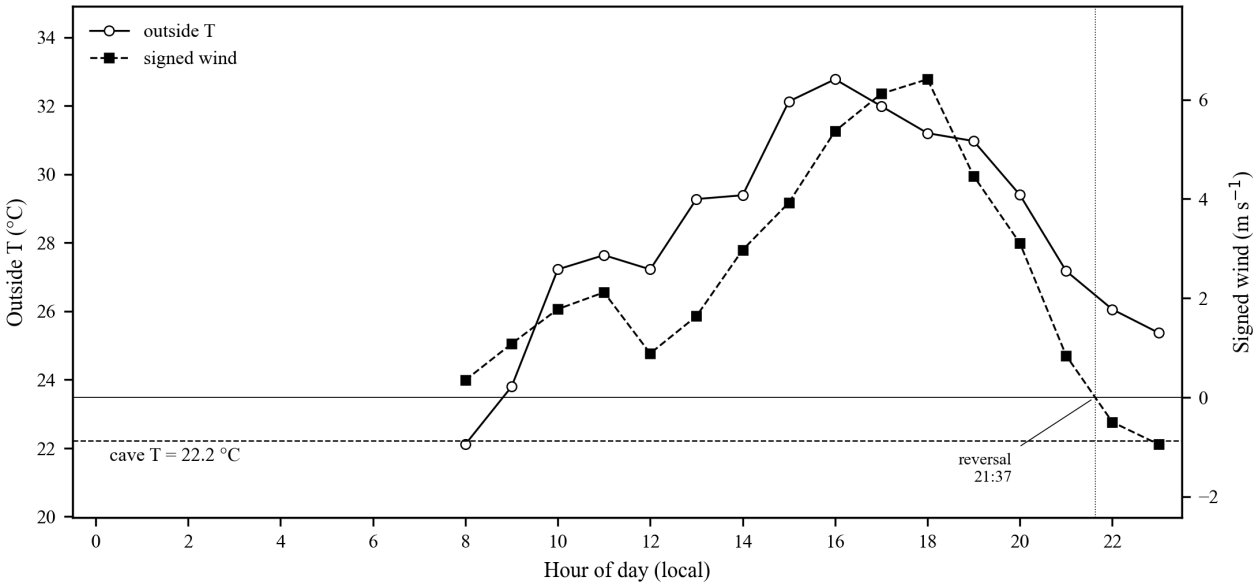

Figure 2. Diurnal composite of outside temperature (blue, left axis) and signed wind (green, right axis), all six observation days pooled by hour of day. Cave temperature of 22.2 °C marked on the temperature axis. Dashed vertical lines mark the times when the mean signed wind crosses zero, at approximately 08:30 and 21:00 local time, coincident with the crossings of outside temperature through cave temperature.

Correlation tests

Three correlation tests cleanly discriminate the two hypotheses (Table 1). The Pearson correlation of signed wind with outside temperature is $r = +0.551$ across 96 samples, with significance below 10^{-8}. The correlation with the chimney form $\mathrm{sign}(\Delta T)\sqrt{|\Delta T|}$ is also $r = +0.551$, as expected since the two predictors are nearly collinear in this dataset. The correlation with dT/dt, used as a proxy for dP/dt, is $r = -0.109$ across 85 samples, within sampling noise of zero at $p > 0.3$. The lag-shifted analysis peaks at lag zero at $r = 0.551$ and falls to $r = 0.533$ at lag $+1$ hour. The cave responds to outside temperature changes with no detectable delay at hourly resolution, the signature of a small cave with thermal mass much smaller than the daily forcing.

The objection that dT/dt is an imperfect proxy for dP/dt is fair at second order. At first order, however, boundary-layer temperature and surface pressure are correlated strongly enough on synoptic timescales that any real barometric driving with synoptic forcing would produce a non-zero correlation here. Warm fronts raise T while P falls. Cold fronts drop T while P rises. The observed $r = -0.109$ is not large enough to support either sign. The chimney correlation, by contrast, is among the cleanest signatures in the cave-ventilation literature.

Signed chimney regression

Fitting Eq. (2) to the full signed dataset by least squares, with C_d fixed at 0.65, leaves a single free parameter, the effective chimney height Δh. The best fit is

$$\Delta h_{\mathrm{fit}} = 48.6 \text{ m } (159 \text{ ft}), \quad R^2 = 0.32.$$

Figure 2 shows the fit in two forms (Fig. 3a, 3b). The left panel plots raw v against ΔT with the chimney curve overlaid. The right panel plots the linearized form $v^2 \,\mathrm{sign}(v)$ against ΔT, which should pass linearly through the origin with slope $2gC_d^2\Delta h/T_o$ if the chimney model holds.

The recovered $R^2 = 0.32$ is moderate. For context, Covington and others (2021) achieved root-mean-squared percentage errors of similar order at Blowing Springs Cave, despite working with three years of one-minute ultrasonic

anemometry rather than 96 hourly samples from a handheld vane. The metrics differ enough that direct numerical comparison should not be pushed too hard, but the qualitative point is that single-parameter symmetric chimney fits in the published literature explain a similar fraction of observed variance, not all of it. The unexplained variance reflects three real physical effects that lie outside the symmetric form of Eq. (2).

The first effect is up-down asymmetry of the buoyancy column. Faimon and Lang (2013) showed that for a U-shaped or stack-configured cave, outflow magnitudes systematically exceed inflow magnitudes under comparable absolute driving forces, through nonlinearity between temperature and air density compounded by a positive feedback on the rising side of the U and a corresponding negative feedback on the descending side. The asymmetry is visible directly in the Blowhole data: peak outflow is 8.0 m/s at $\Delta T \approx +4.9$ °C, while peak inflow is only 2.1 m/s at $\Delta T \approx -0.9$ °C. A symmetric chimney model with a single Δh cannot fit both envelopes at once. The least-squares fit averages them, which necessarily underpredicts the outflow extremes and overpredicts the inflow extremes. This is the dominant source of scatter in Fig. 2.

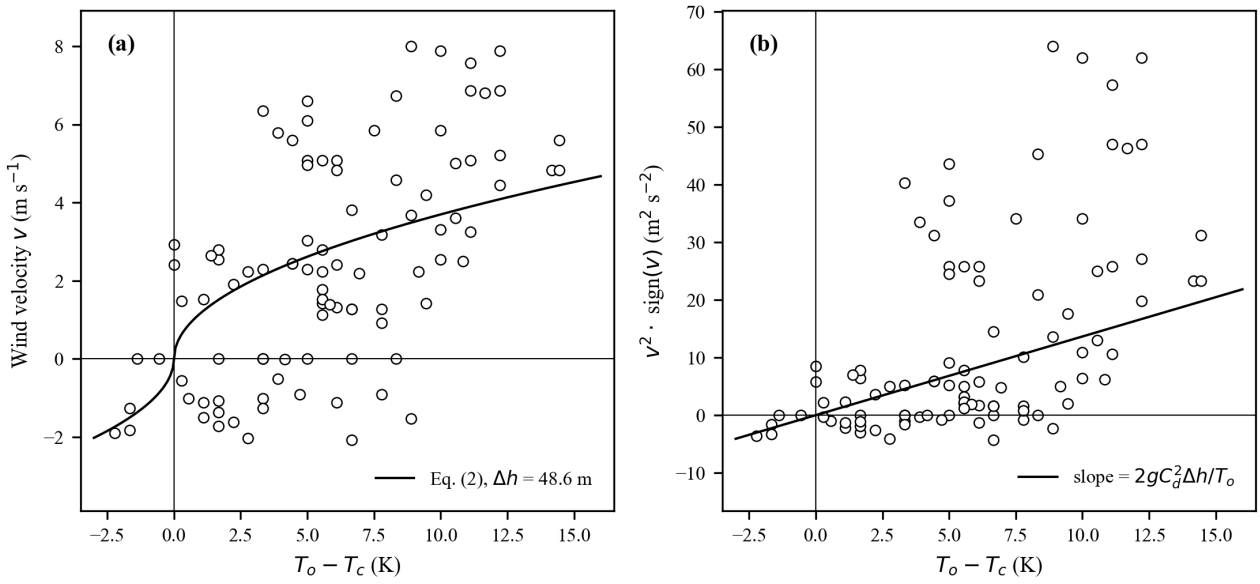

Figure 3. Signed chimney regression. (a) Signed wind velocity against $\Delta T = T_o - T_c$ with the best-fit chimney model curve (Eq. 2) overlaid, $\Delta h = 48.6$ m, $C_d = 0.65$, $R^2 = 0.32$. (b) Linearized form: $v^2 \mathrm{sign}(v)$ against ΔT, which should pass linearly through the origin with slope $2gC_d^2\Delta h/T_o$ if the chimney model holds.

The second effect is thermal lag of the cave interior. The effective T_c actually felt by the flowing column is not a single instantaneous number. Air entering the cave on a hot afternoon does not reach the deep-cave temperature for tens of meters of travel, and the entry passages warm during the day and cool overnight on a thermal-relaxation length of order 100 m (Gabrovšek, 2023; Sedaghatkish and others, 2024). The effective driving ΔT is therefore mildly less than $(T_o - 22.2\ ^\circ C)$ during the most rapid afternoon ramp, and mildly greater than that value during the overnight inflow regime when the entry passages are still warm. Both effects scatter the points away from the single curve in Fig. 2 in a predictable way, producing concave loops in time.

The third effect is surface-wind augmentation. Gabrovšek and others (2021) showed at Postojna Cave that surface wind across irregular topography produces inter-entrance pressure differences that augment or oppose the chimney flow. For Blowhole's small entrance tucked at the bottom of a draw, the entrance is sheltered from most wind directions, and the contribution should be small. It is, however, uncorrelated with ΔT and so contributes purely to the scatter rather than to any systematic bias.

The key point about these three effects, taken as a whole, is that every one of them blurs a chimney signal without producing a spurious chimney signal where none exists. Their net effect on the diagnosis is to lower the achievable R^2, not to mimic chimney behavior in a cave actually driven by some other mechanism.

Topographic relief

The cave entrance sits at 612 m (2,006 ft) in a small draw. Within 200 m of the entrance, the highest ground reaches 618 m (2,029 ft), for 7 m (23 ft) of relief. Within 500 m and 1 km, the maximum is 621 m (2,038 ft), for 10 m (33 ft) of relief. Within 2 km it reaches 637 m (2,089 ft), for 25 m (83 ft) of relief. Within 3 km the maximum is 639 m (2,096 ft), for 27 m (90 ft) of relief (Table 2). The topographic context is shown in Fig. 4.

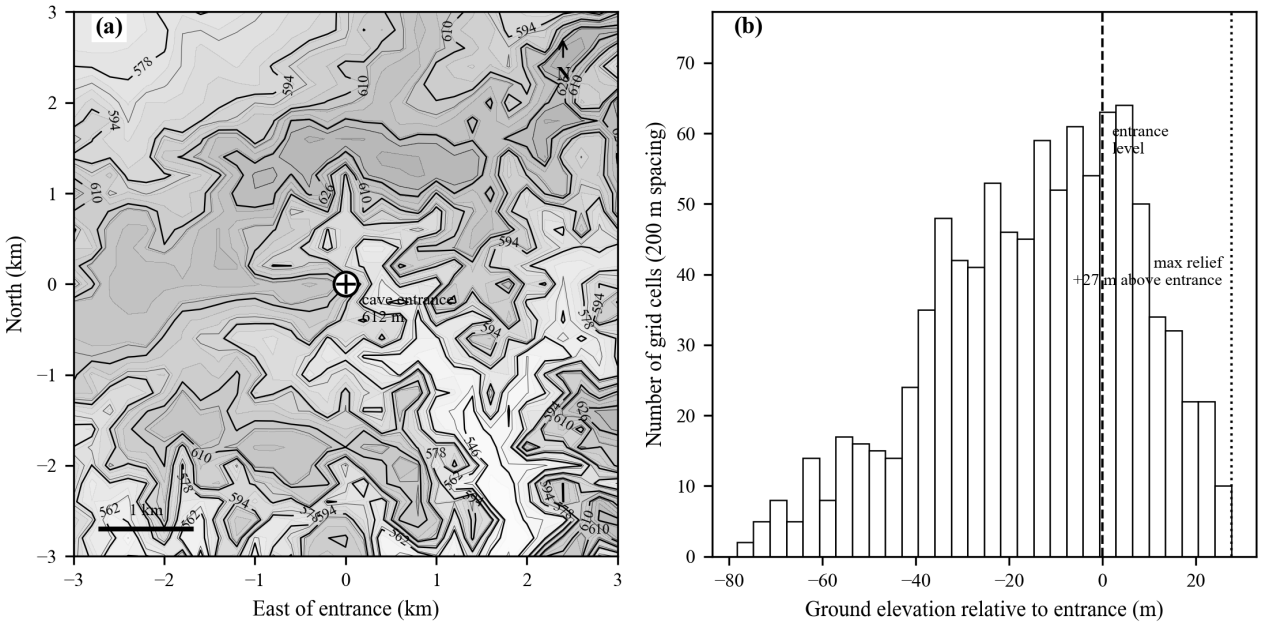

Figure 4. Local topography around Blowhole Cave entrance. (a) Shaded-relief map of a 6 km by 6 km area centered on the cave entrance, sampled from the USGS 3DEP National Elevation Dataset at 200 m grid spacing. Cave entrance marked with the standard cave-entrance symbol. Contour interval 8 m (25 ft). (b) Histogram of nearby ground elevations relative to the cave entrance, all 961 grid samples. Maximum relief above the entrance within 3 km is 27 m (90 ft).

The Edwards Plateau in this part of Edwards County is gently dissected, with the entrance in a small draw and the surrounding plateau surface only 5 to 11 m higher locally. A naive reading of the chimney model would conclude that surface topography supplies at most 27 m (90 ft) of Δh, which is far less than the 49 m (159 ft) the regression recovered. The naive reading is incomplete in a way addressed below.

The comparison with published chimney caves is informative. Covington and others (2021) report Blowing Springs Cave entrances separated by about 25 m of elevation, comparable to the maximum surface relief available within 2 km of the Blowhole entrance. The Postojna Cave system studied by Gabrovšek and others (2021) has $\Delta h \approx 40$ m between the openings considered. Both are caves where the chimney column lies primarily above ground, so that the surface elevation difference between entrances is the effective chimney height in Eq. (1). Blowhole has only about 10 m of available surface relief within 1 km of the entrance, which is apparently insufficient. The resolution lies inside the cave itself.

Cave-interior chimney column

The cave description from the Project Deep field notes contains the crucial datum. The total surveyed depth is 102 m (336 ft). That depth is distributed across a series of vertical airspaces: a 6 m entrance drop, a chimney climbing to a

higher room, a 24 m pit, additional drops into deep rooms 18 to 21 m tall. The cave is, mechanically, a stack of connected vertical columns extending 102 m below the entrance.

What matters for a chimney is the vertical separation between the warm and cool columns of air, not how that separation is distributed between above grade and below grade. Cold dense cave air filling 102 m of vertical extent inside the cave produces hydrostatic head exactly the same way a 102 m above-ground chimney does. Equation (1) responds only to Δh and ΔT, and is indifferent to where the column sits relative to grade. The same principle allows mine shafts and underground laboratories to operate as effective chimneys with no above-ground stack at all.

The geometric requirement is that the cave must have two openings at different elevations, or one opening plus a connection to the surface through fractures sufficient to pass air. Blowhole has only one mapped entrance. For the cave-interior column to act as a chimney, there must be a second exchange point somewhere, whether a fissure, a crack network, a breakdown gap, or a small undiscovered opening through which the upper end of the cave column communicates with the outside.

With $\Delta h = 102.3$ m and the measured ΔT at the time of the strongest gust, equal to $(31.1 - 22.2) = 8.89$ °C, Eq. (2) predicts a peak velocity of

$$v_{\text{pred}} = 0.65 \sqrt{2 \times 9.81 \times 102.3 \times \frac{8.89}{304.3}} = 4.98 \text{ m/s } (980 \text{ ft/min}).$$

The cave-interior column alone, with no surface contribution, accounts for 4.98 out of 8.00 m/s, or 62 percent of the peak observed velocity. Equivalently, it accounts for $(4.98/8.00)^2 = 39$ percent of the buoyancy head required at peak. The cave's own deep pits are doing most, but not quite all, of the work.

Peak-flow observation

The strongest single observed flow, 8.00 m/s at 17:00 on the 28th with outside temperature 31.1 °C, is faster than the cave-interior column alone predicts. Inverting Eq. (2) for that one observation gives a required Δh of about 264 m, which is 2.6 times the cave's surveyed interior depth, or equivalently a velocity factor of 1.61 above the prediction since $v \propto \sqrt{\Delta h}$. The cave's 102 m internal column predicts a peak of about 5.0 m/s under the same ΔT, so the cave-alone model accounts for 62 percent of the observed peak velocity.

The discrepancy is on the order of what would be produced by a less conservative discharge coefficient than the $C_d = 0.65$ used throughout this analysis (a value of 0.85 is closer to the geometry of a small entrance opening into much wider passages, per Massey 1989), by the up-direction asymmetry quantified by Faimon and Lang (2013) for U-shaped caves, by vena-contracta enhancement at the anemometer location, or by some combination. The single observation does not by itself constrain which of these effects is responsible. I note the discrepancy here as an observation worth follow-up, not as a quantitative argument for any specific cause. A modern repeat of the 1976 measurements with calibrated anemometry and full-cycle sampling would resolve which effect dominates.

Rejection of the barometric hypothesis

The barometric hypothesis is rejected on six independent grounds.

First, wrong predictor. Wind correlates strongly with T_o ($r = +0.551$, $p < 10^{-8}$) and not at all with dT/dt ($r = -0.11$, $p > 0.3$). A Helmholtz cave produces the opposite ranking. Gomell and Pflitsch (2022) confirmed at Wind Cave and Jewel Cave that pressure-derivative quantities are the appropriate predictor for barometric caves. Their absence at Blowhole is diagnostic.

Second, wrong phase. Sign reversals at Blowhole lock to time of day at 08:30 and 21:00 across all five observation days spanning two separate weeks. The atmospheric solar tide does have a semidiurnal pressure component at mid-latitudes, with amplitude around 1 to 2 hPa, but that amplitude is far too small to drive 7.6 m/s through a 0.139 m²

opening in a cave of any plausible size. Pflitsch and others (2010) document for Wind and Jewel Caves that barometric airflow direction follows synoptic pressure systems on multi-day timescales with no diurnal lock.

Third, wrong volume requirement. Inverting Eq. (3) gives the cave volume needed to produce the observed peak velocity from a representative diurnal pressure swing of 3 hPa over 12 hours, or dP/dt of 6.9×10^{-3} Pa per second. The result is

$$V = \frac{|v| A P}{|dP/dt|} = \frac{8.0 \times 0.139 \times 1.013 \times 10^{5}}{6.9 \times 10^{-3}} \approx 1.6 \times 10^{7}\ \mathrm{m}^3.$$

This is roughly 1,100 times the surveyed cave volume, which I estimate at 1.4×10^{4} m³ from the survey notes. As a cross-check on the calculation, this same volume-from-breathing inversion of Eq. (3) is the technique the National Park Service uses to estimate Jewel Cave's total air volume from the magnitude of its barometric breathing at the entrance (National Park Service, 2024). The estimate is approximately 2.3×10^{8} m³ of total cave-air volume, of which the surveyed 355 km of passages account for only 3 to 5 percent. The technique gives self-consistent numbers in caves where the barometric mechanism actually operates. Jewel Cave's surveyed length is roughly 2,000 times that of Blowhole, and even Jewel Cave's inferred total volume is only about 14 times what would be required at Blowhole to make the barometric explanation work at observed flow magnitudes. For the barometric mechanism to be responsible for Blowhole's airflow, Blowhole would have to hide an undiscovered passage volume comparable to one of the longest caves in the world.

Fourth, the cave-temperature crossing. The flow reverses precisely when outside temperature crosses the independently measured cave temperature of 22.2 °C. This is a parameter-free prediction of the chimney model, with no fitted variable, and it is among the cleanest signatures available in cave-airflow analysis. Barometric flow predicts no such temperature-locked reversal.

Fifth, wrong morphological class. Documented barometric caves of comparable airflow magnitude (Wind Cave and Jewel Cave the most thoroughly characterized) share two features: total cave-air volume on the order of 10^{8} m³, and surveyed volume-to-entrance-area ratio on the order of 10^{7} to 10^{8} m. Blowhole's volume-to-area ratio is $1.4 \times 10^{4} / 0.139 \approx 10^{5}$ m, two to three orders of magnitude smaller than the canonical barometric morphology. Even with generous allowance for unsurveyed extensions, Blowhole would have to be morphologically reclassified into a wholly different category of cave to support the barometric explanation.

Sixth, net mass-balance anomaly. Integrating the signed velocity over the 96 sampled hours gives a net signed throughput of approximately $+1.15 \times 10^{5}$ m³, net outflow over the observation window. Outflow events sum to 1.28×10^{5} m³. Inflow events sum to only 1.32×10^{4} m³. A purely barometric cave must conserve mass through its single opening on any timescale long compared to the dominant forcing period. For synoptic forcing of 12 to 36 hour periods, mass balance through a single opening should be approached within a few days. The observed 10:1 outflow-to-inflow imbalance over five days is not consistent with single-opening mass balance under synoptic-scale forcing. It is, however, exactly consistent with a chimney system in which air enters at an unsurveyed upper opening and exits at the surveyed lower entrance during the summer regime, with the reverse pattern in winter. One caveat is that the 1976 measurements were made predominantly during waking hours on most days, biasing the sample toward times when summer outflow dominates. The 9th-10th block is the exception, a continuous 24-hour record, and it still shows roughly 4:1 outflow-to-inflow by integrated volume. Sampling bias alone cannot account for the imbalance.

Discussion

Implications for the cave-ventilation literature

Two implications of this analysis are worth flagging for the broader cave-ventilation literature. The first is that effective chimney height Δh in Eq. (1) need not equal the inter-entrance surface elevation difference when the cave has

substantial vertical interior relief. At Blowhole, the 102 m of internal vertical extent surveyed in the cave is more than sufficient to drive observed flow magnitudes without invoking any surface-to-surface elevation difference at all. In published chimney caves where Eq. (2) has been validated (Blowing Springs at $\Delta h \approx 25$ m, Postojna at ≈ 40 m), inter-entrance surface elevation difference is the dominant contribution. Blowhole occupies a different point in parameter space: a cave whose effective chimney height is dominated by below-grade vertical extent. This morphological class deserves explicit recognition.

The second is that the volume-from-breathing inversion of Eq. (3), which Gomell and Pflitsch (2022) and others use to estimate hidden cave volume from barometric flow magnitude, provides an equally useful test in the opposite direction. If the calculation gives a volume that is implausibly larger than the surveyed cave, the cave is not barometric. At Blowhole the inversion gives 1.6×10^7 m³, about 1,100 times the surveyed volume and well into the range where the barometric explanation collapses. The test is computationally trivial and should be standard practice when classifying caves of small to intermediate size.

Limitations

The principal limitation of this analysis is the absence of simultaneous barometric pressure data. The chimney model passes every available test against the temperature data, but a direct test against dP/dt would settle the diagnosis the cleanest way. A second limitation is the moderate $R^2 = 0.32$ of the chimney regression. As discussed above, the unexplained variance is consistent with known physical effects that lie outside the symmetric form of Eq. (2). A modern repeat of the 1976 measurements with ultrasonic anemometry, co-located barometry, and interior temperature logging at multiple depths would likely lift R^2 substantially, but the qualitative diagnosis is robust to instrumentation upgrades. A third limitation is the single peak observation discussed under Peak-flow observation above, which exceeds the cave-interior column prediction by a factor of 1.6 in velocity. Resolving whether the excess reflects a less conservative discharge coefficient, the Faimon-Lang outflow nonlinearity, vena-contracta enhancement, or an as-yet-unidentified additional exchange path requires new field measurements rather than further analysis of the 1976 data.

Recommended follow-up

Three further measurements would close the remaining methodological loose ends. The first is a co-located high-resolution barometer at the entrance for one week, then re-running the airflow regression against dP/dt at the surface and against the cave-to-surface pressure gradient, following the Gomell and Pflitsch (2022) protocol. The chimney model predicts essentially zero correlation. The barometric model predicts $R^2 > 0.5$. This single dataset would lock in the diagnosis against any methodological objection. The second is continuous interior temperature logging at multiple depths to characterize the thermal-relaxation length of Sedaghatkish and others (2024) and refine the effective T_c used in Eq. (2). The third is a calibrated full-cycle anemometer record across a complete diurnal cycle, including the morning and evening reversal transitions, to resolve the up-down asymmetry quantified by Faimon and Lang (2013) and to determine whether the single peak observation of 8 m/s is representative or anomalous.

Conclusions

Blowhole Cave is a thermal-chimney cave, not a barometric cave. The airflow data fit the buoyancy-driven two-entrance model in every testable respect: sign of flow, phase of reversals, predictor correlation, and quantitative magnitude scaling. The barometric and large-volume hypothesis fails on six independent grounds, including failure of the pressure-gradient predictor criterion that Gomell and Pflitsch (2022) established as diagnostic for barometric systems, and a hidden-volume requirement of order 10^3 times the surveyed cave volume.

The central quantitative result is that the cave's own 102 m (336 ft) of internal vertical relief is more than sufficient to drive the observed airflow. The deep pits and stacked vertical rooms function as the cold-air leg of the chimney. The single-parameter chimney regression recovers $\Delta h = 49$ m, comfortably less than the surveyed cave depth and consistent with Eq. (2) given a conservative discharge coefficient. Surface topography around the entrance is gentle, with only 27 m (90 ft) of relief within 3 km, but the cave is not topographically limited because the buoyancy column

extends below grade. This configuration sets Blowhole apart from the better-studied chimney caves in the published literature (Blowing Springs Cave at $\Delta h \approx 25$ m, Postojna Cave at ≈ 40 m), where inter-entrance elevation difference is provided primarily above ground.

The sharpest single piece of evidence is that flow reverses sign precisely when outside temperature crosses cave temperature. This is a parameter-free prediction of the chimney model: no fitted variable was used to produce it, and no other published cave-ventilation mechanism reproduces it. The 1976 field interpretation by the Project Deep survey team was correct and is quantitatively confirmed. The observation that very strong currents of air flow from the cave during the afternoon and evening, and that air enters the cave during the night and morning, and that the present entrance is therefore a lower entrance, is exactly what the chimney equation predicts given the cave's measured geometry and the cave-versus-outside temperature regime.

Acknowledgments

I thank the 1976 Project Deep survey team for the original cave description and meteorological field notes that made this analysis possible, and the cave's landowners for access during the original measurement campaign. The USGS 3D Elevation Program provides the topographic data used in the surface analysis. The author has no competing financial interests.

Tables

Predictor	Pearson r	Sample size n	Significance p	Favored hypothesis
T_o (outside temperature)	$+0.551$	96	$< 10^{-8}$	Chimney
$\operatorname{sign}(\Delta T)\sqrt{\lvert\Delta T\rvert}$ (chimney form)	$+0.551$	96	$< 10^{-8}$	Chimney
dT/dt (barometric proxy)	-0.109	85	> 0.3	Neither
[**Table 1.** Pearson correlation of signed entrance airflow against three candidate predictors. The chimney form is $\operatorname{sign}(\Delta T)\sqrt{\lvert\Delta T\rvert}$. The dT/dt predictor is a proxy for dP/dt when pressure data are unavailable. Sample sizes differ because dT/dt requires a central difference that drops the first and last samples of each day.]				

Table 2. Maximum surface elevation and corresponding relief above the cave entrance within concentric radii. Data from USGS 3D Elevation Program (3DEP) National Elevation Dataset, sampled on a 31-by-31 grid at 200 m spacing centered on 29.7336° N, 100.6342° W. Cave entrance elevation is 612 m (2,006 ft).

Radius from entrance	Highest ground (m)	Highest ground (ft)	Relief above entrance (m)	Relief above entrance (ft)
0.2 km	618	2,029	7	23
0.5 km	621	2,038	9	30
1.0 km	621	2,038	9	30
2.0 km	637	2,089	25	83
3.0 km	639	2,096	27	90

Table 3. Symbols used in this paper.

Symbol	Meaning	Value or units
T_o	Outside air temperature	K (or °C as noted)
T_c	Cave air temperature	295.4 K (22.2 °C)
ΔT	$T_o - T_c$	K
Δh	Effective vertical separation of buoyancy columns	m
ρ_o	Outside-air density	kg m^{-3}
g	Gravitational acceleration	9.80665 m s^{-2}
C_d	Discharge coefficient at entrance restriction	0.65 (this study)
f	Darcy-Weisbach friction factor	dimensionless
L, D_H	Flow-path length, hydraulic diameter	m
A	Entrance cross-sectional area	0.139 m²

v	Entrance wind velocity, signed (+ outflow)	m s^{-1}
V	Internal cave volume	m^3
P	Atmospheric pressure	Pa

References

Christoforou, C.S., Salmon, L.G., and Cass, G.R., 1996, Air exchange within the Buddhist cave temples at Yungang, China: Atmospheric Environment, v. 30, no. 23, p. 3995–4006, https://doi.org/10.1016/1352-2310(96)00123-9.

Covington, M.D., Knierim, K.J., Young, H.A., Rodriguez, J., and Gnoza, H.G., 2021, The impact of ventilation patterns on calcite dissolution rates within karst conduits: Journal of Hydrology, v. 593, article 125824, https://doi.org/10.1016/j.jhydrol.2020.125824.

de Freitas, C.R., Littlejohn, R.N., Clarkson, T.S., and Kristament, I.S., 1982, Cave climate: Assessment of airflow and ventilation: Journal of Climatology, v. 2, no. 4, p. 383–397, https://doi.org/10.1002/joc.3370020408.

Faimon, J., and Lang, M., 2013, Variances in airflows during different ventilation modes in a dynamic U-shaped cave: International Journal of Speleology, v. 42, no. 2, p. 115–122, https://doi.org/10.5038/1827-806X.42.2.3.

Gabrovšek, F., 2023, How do caves breathe: The airflow patterns in karst underground: PLOS ONE, v. 18, no. 4, e0283767, https://doi.org/10.1371/journal.pone.0283767.

Gabrovšek, F., Kukuljan, L., and Covington, M.D., 2021, The relative importance of wind-driven and chimney effect cave ventilation: Observations in Postojna Cave (Slovenia): EarthArXiv preprint, https://doi.org/10.31223/x5r622.

Gomell, A.K., and Pflitsch, A., 2022, Airflow dynamics in Wind Cave and Jewel Cave: How do barometric caves breathe?: International Journal of Speleology, v. 51, no. 3, p. 165–180, https://doi.org/10.5038/1827-806X.51.3.2437.

Lewis, W.C., 1991, Atmospheric pressure changes and cave airflow: A review: National Speleological Society Bulletin, v. 53, no. 1, p. 1–12.

Massey, B.S., 1989, Mechanics of Fluids, 6th ed.: London, Van Nostrand Reinhold, 599 p.

National Park Service, 2024, Jewel Cave National Monument: Cave statistics and exploration: U.S. Department of the Interior, https://www.nps.gov/jeca/learn/historyculture/jewel-cave-statistics.htm [accessed May 16, 2026].

NOAA National Centers for Environmental Information, 2024, Climate at a Glance: County time series, Edwards County, Texas, mean annual temperature 1895–2024: https://www.ncei.noaa.gov/access/monitoring/climate-at-a-glance/county/ [accessed May 16, 2026].

Passmore, G., 2023, Mathematical modeling of cave breathing dynamics: An analysis of airflow, barometric pressure, and temperature in Blowhole Cave, West Texas: ResearchGate preprint 375994359, https://www.researchgate.net/publication/375994359 [accessed May 16, 2026].

Pate, D., Cross, J., and Grubbs, A., 1979, Blowhole Cave map: Texas Speleological Survey, https://www.texasspeleologicalsurvey.org/deeplong/deeplong-maps/Blowhole.pdf [accessed May 20, 2026].

Pflitsch, A., Wiles, M., Horrocks, R., Piasecki, J., and Ringeis, J., 2010, Dynamic climatologic processes of barometric cave systems using the example of Jewel Cave and Wind Cave in South Dakota, USA: Acta Carsologica, v. 39, no. 3, p. 449–462, https://doi.org/10.3986/ac.v39i3.75.

Sartor, J.D., and Lamar, D.L., 1962, Meteorological-geological investigations of the Wupatki Blowhole system: Santa Monica, California, RAND Corporation Memorandum RM-3139-RC, 53 p.

Sedaghatkish, A., Pastore, C., Doumenc, F., Luetscher, M., and Jeannin, P.-Y., 2024, Modeling heat transfer for assessing the convection length in ventilated caves: Journal of Geophysical Research: Earth Surface, v. 129, no. 6, article e2024JF007646, https://doi.org/10.1029/2024JF007646.

Texas State Historical Association, 2024, Edwards County profile: Texas Almanac, https://www.texasalmanac.com/places/edwards-county [accessed May 16, 2026].

Wigley, T.M.L., and Brown, M.C., 1976, The physics of caves, *in* Ford, T.D., and Cullingford, C.H.D., eds., The Science of Speleology: London, Academic Press, p. 329–358.